Environmental Pollution 158 (2010) 1015–1022

Contents lists available at ScienceDirect

Environmental Pollution

journal homepage: www.elsevier.com/locate/envpol

Analysis of a Farquhar-von Caemmerer-Berry leaf-level photosynthetic rate model for *Populus tremuloides* in the context of modeling and measurement limitations

Kathryn E. Lenz [a,*], George E. Host [b], Kyle Roskoski [b], Asko Noormets [c,1], Anu Sôber [d], David F. Karnosky [c]

[a] Department of Mathematics and Statistics, University of Minnesota Duluth, 10 University Drive, Duluth, MN 55812, USA
[b] Natural Resources Research Institute, University of Minnesota Duluth, 5013 Miller Trunk Highway, Duluth, MN 55811, USA
[c] School of Forestry Resources and Environmental Science, Michigan Technological University, 1400 Townsend Drive, Houghton, MI 49931, USA
[d] Institute of Ecology and Earth Sciences, University of Tartu, 40 Lai Str. 51005, Tartu, Estonia

A photosynthetic rate model is parameterized for Populus tremuloides and evaluated based on its ability to predict dependent as well as independent data.

ARTICLE INFO

Article history:
Received 11 August 2009
Accepted 17 August 2009

Keywords:
Photosynthetic rate model
Populus tremuloides
Parameterization
Validation

ABSTRACT

The balance of mechanistic detail with mathematical simplicity contributes to the broad use of the Farquhar, von Caemmerer and Berry (FvCB) photosynthetic rate model. Here the FvCB model was coupled with a stomatal conductance model to form an [A,g_s] model, and parameterized for mature *Populus tremuloides* leaves under varying CO_2 and temperature levels. Data were selected to be within typical forest light, CO_2 and temperature ranges, reducing artifacts associated with data collected at extreme values. The error between model-predicted photosynthetic rate (A) and A data was measured in three ways and found to be up to three times greater for each of two independent data sets than for a base-line evaluation using parameterization data. The evaluation methods used here apply to comparisons of model validation results among data sets varying in number and distribution of data, as well as to performance comparisons of [A,g_s] models differing in internal-process components.

1. Introduction

The widely accepted, steady-state photosynthetic rate model of Farquhar, von Caemmerer and Berry (1980), the FvCB model, relates C_3 leaf gas exchange data to underlying limitations to photosynthesis at the leaf-tissue level due to the activity of Rubisco, regeneration of RuBP and stomatal conductance. The model achieves a useful balance between mechanistic detail and mathematical simplicity. Various modifications to the model have been developed in order to extend its responsiveness to a wide range of environmental conditions (Hikosaka et al., 2006; Rogers and Humphries, 2000) water and nutrient stress (Dewar, 2002; Kubiske et al., 2002), and elevated CO_2 and O_3 concentrations (Karnosky et al., 2003; Kull et al., 1996; Martin et al., 2000, 2001; Reich, 1983).

As noted by Farquhar, von Caemmerer and Berry (2001), the FvCB model does not include all mechanisms contributing to photosynthetic rate. Instead it represents an intelligent, simplified blend of processes occurring at the chloroplast level. Extrapolation of the model to the leaf-level, however, can result in erroneous assumptions about homogeneity of photosynthetic activity throughout the leaf, gas conductances and other internal processes (Flexas et al., 2008; Schurr et al., 2006). In order to predict photosynthetic rate from external rather than internal CO_2 concentration, the FvCB model is coupled with a stomatal conductance model, often of the Ball-Berry (Ball et al., 1987) or Leuning (Leuning, 1995) type, forming an [A,g_s] model.

Different strategies for calibrating the non-linear FvCB model, with its interdependent parameters, can lead to different sets of parameter values (see e.g. Sharkey et al., 2007). For example, Dubois et al. (2007) showed that, using standard parameterization methods, the assumed value of the A/C_i transition point alone can significantly influence the resulting estimates of V_{cmax}, J_{max} and R_d. (See the Appendix for symbol definitions and units.) Moreover, parameters for these components are typically determined as optimal regression fits to data and such fits can be sensitive to data distribution, inaccuracies and bias.

Unrecognized limitations and bias of instrumentation can also be misleading (Long and Bernacchi, 2003; Long et al., 1996). Estimates of respiration, CO_2 compensation point, V_{cmax} and J_{max} can all vary significantly with instrumentation and techniques

* Corresponding author. Tel.: +1 218 726 7216; fax: +1 218 726 8399.
E-mail addresses: klenz@d.umn.edu (K.E. Lenz), ghost@nrri.umn.edu (G.E. Host), kroskosk@d.umn.edu (K. Roskoski), anoorme@ncsu.edu (A. Noormets), anu.sober@ut.ee (A. Sôber).
[1] Current address: Department of Forestry and Environmental Resources, North Carolina State University and Southern Global Change Program, USDA Forest Service, Raleigh, NC 27695-7260, USA.

0269-7491/$ – see front matter © 2009 Elsevier Ltd. All rights reserved.
doi:10.1016/j.envpol.2009.08.004

(Bernacchi et al., 2002; Ethier and Livingston, 2004; Singsaas et al., 2003). Data collected at extreme C_a levels within a gas exchange chamber are proportionately more affected by measurement error, imprecision and CO_2 leakage and diffusion than when chamber C_a levels are close to external C_a levels (Long and Bernacchi, 2003; McDermitt et al., 1989; Rodeghiero et al., 2007). Because of the technique by which A is measured, CO_2 leaking or diffusing into the chamber at low chamber C_a reduces apparent A, while CO_2 leaking out of the chamber at high chamber C_a increases apparent A. Also the use of C_i in place of C_c introduces bias in estimation of V_{cmax} and J_{max} (Singsaas et al., 2003), though the difference between C_i and C_c is difficult to predict (Flexas et al., 2007, 2008).

Measurements to estimate J_{max} are often made at chamber $C_a = 2000$ ppm to ensure that CO_2 is saturating and hence photosynthesis is RuBP regeneration limited. However at very high cuvette C_a there can be measurement problems related to stomatal closure in illuminated leaves (Niinemets et al., 1999). Also, phosphate availability may curb RuBP regeneration (Niinemets et al., 1999; Sharkey, 1985), leading to underestimation of J_{max}.

This study parameterized and validated a coupled [A,g_s] model using leaf-level A/C_i data with the goal of predicting A at growth C_a levels while seeking to minimize measurement effects and unmodeled photosynthetic rate dynamics. Validation was based on the [A,g_s] model's predictions of measured A values for dependent (i.e. parameterization) and independent data sets. Parameterization and validation were limited to leaf-level photosynthetic rate for healthy, mature *P. tremuloides* Michx. sun leaves with environmental conditions typical of aspen forests, in the absence of water and nutrient stress.

2. Methods of model development

2.1. Mathematical model

In Farquhar et al. (1980) steady-state C_3 leaf photosynthetic carbon assimilation rate A is driven by intercepted light, CO_2, temperature, and humidity as well as internal leaf processes. Photosynthetic rate is assumed to be limited either by Rubisco-catalyzed carboxylation, the regeneration of RuBP controlled by electron transport rate, or the regeneration of RuBP controlled by the rate of triose-phosphate utilization, TPU. No evidence of TPU limitation was found in the data (Long and Bernacchi, 2003; von Caemmerer, 2000). Thus $A = \min\{A_c, A_j\}$, where Rubisco-limited A is given by

$$A_c = \frac{V_{c,max}(C_i - \Gamma^*)}{C_i + K_m} - R_d, \quad (1)$$

where $K_m = K_c(1 + \frac{O_i}{K_o})$, and RuBP regeneration limited A is given by

$$A_j = \frac{J(C_i - \Gamma^*)}{4.5C_i + 10.5\Gamma^*} - R_d \quad (2)$$

As in Harley and Tenhunen (1991), dark respiration was expressed as an Arrhenius function of temperature of the form

$$R_d = \exp(c)\exp(-\Delta H_a/(RT_k)) \quad (3)$$

The temperature dependencies for Γ^* and K_m were drawn from Bernacchi et al. (2002). The parameters V_{cmax} and J_{max} were modeled as in Harley and Tenhunen (1991), Harley et al. (1992b) and Medlyn et al. (2002) by peaked temperature functions of the form

$$P(T_k) = P_{opt}\left(\frac{\Delta H_d \exp\left(\frac{\Delta H_a(T_k - T_{opt})}{T_k R T_{opt}}\right)}{\Delta H_d - \Delta H_a\left(1 - \exp\left(\frac{\Delta H_d(T_k - T_{opt})}{T_k R T_{opt}}\right)\right)}\right), \quad (4)$$

where $P(T_k)$ is the value of the parameter at temperature T_k, P_{opt} is the maximum value of the parameter and T_{opt} is the temperature at which P_{opt} is achieved.

The rate of electron transport, J, was related to J_{max} according to

$$\Theta_{PSII}J^2 - (Q_2 + J_{max})J + Q_2 J_{max} = 0 \quad (5)$$

The temperature dependences of Θ_{PSII} and Q_2 were those of Bernacchi et al. (2003) for growth temperature 14 °C.

As implemented in LI-6400 (equations from Farquhar and Sharkey, 1982; and Farquhar and von Caemmerer, 1982),

$$C_i = \frac{(g_{tc} - E/2000)C_s - A}{g_{tc} + E/2000}, \quad (6)$$

for $C_s = \frac{F}{100S}C_r - A\Big/\frac{F}{100S} + 0.001E$, where F is air flow rate and S is leaf surface area inside the cuvette. In this study, $g_{tc} = \left(\frac{1.6}{g_s} + \frac{1.37(0.5)}{1.42}\right)^{-1}$, where g_s has the form

$$g_s = \frac{a_1(A + R_d)}{C_i(1 + \frac{D_s}{D_o})} \quad (7)$$

This is a variation of the basic Ball-Berry-Leuning g_s model (Leuning, 1995).

2.2. Parameterization data

This study differs from previous work in the selection criteria developed and applied to data prior to parameterization. The intent was to use real-world data sets filtered to avoid or reduce uncertainty due to unmodeled photosynthesis dynamics associated with leaf-age, leaf-health, low stomatal conductance, photoinhibition, water stress or nutrient availability. The data were also filtered to reduce the effects of potential instrumentation-induced errors at very low or very high values of C_r. Model components were parameterized primarily to high-light data with C_r close to C_a growth levels, where steady-state photosynthesis measurements are most likely representative of photosynthesis in the field.

The data used for parameterization in this study were collected as part of the Aspen FACE project (Dickson et al., 2000; Karnosky et al., 2003), located at 45°30′ N, 89°30′ W. Leaf-level data were collected from *P. tremuloides* clone 216 growing in open-air conditions with exposure to elevated (550 ppm) and ambient (360 ppm) levels of CO_2 during the 1998 and 2000 growing seasons. All measurements were made using an LI-6400 portable open gas exchange photosynthesis system (LI-COR, 1998, 2006). Only data for leaves within a Leaf Plastochron Index (LPI) range of approximately 9–26 were used. This range includes predominately recently mature and mature leaves. Kull et al. (1996) placed leaf maturation, based on chlorophyll content, at about LPI 8, while Noormets et al. (2001a) placed leaf maturation at about LPI 11. Because photosynthetic rate capacity may diminish in over-mature leaves and in leaves damaged by ozone (Kim and Lieth, 2003; Reich, 1983; Schultz, 2003; Niinemets et al., 2005), data for clearly over-mature or damaged leaves were excluded according to LPI and cut-off values for A. For $Q \geq 1000$ μmol m^{-2} s^{-1}, A was required to be at least 15 μmol m^{-2} s^{-1} when $C_r > 300$ ppm and at least 20 when $C_r > 400$ ppm. Data for which measured g_s averaged less than 0.3 when C_i was between 145 and 500 ppm were also excluded as low g_s measurements could occur for various reasons associated with unmodeled leaf-tissue behavior (Farquhar and Sharkey, 1982; Leuning, 1995; Mott and Buckley, 2000; Noormets et al., 2001b).

The full parameterization data set, the [A,g_s]-data, was the union of the first three limited data sets listed in Table 1. A large proportion of the [A,g_s]-data were for C_r levels between 340 and 560 ppm, since predicting A for ambient growth conditions was of highest priority. All of the data for $C_r < 400$ ppm was for leaves grown at day-time C_a close to 350 ppm and all of the data for $C_r > 400$ ppm was for leaves grown under elevated day-time C_a, about 550 ppm. The A_c-data consisted of the FACE-1998_A data for which $C_r \leq 360$ ppm and the FACE-1998_B data for which A appeared to be RuBP carboxylation-limited based on A/C_i curves. The A_j-data comprised the low-light FACE-2000 data, the FACE-1998_A data for which C_r was above 540 ppm and the FACE-1998_B data for which C_i was at or above the cross-over point.

The V_{cmax} parameterization data set (V-data) consisted of the A_c-data for which C_r was approximately 250–530 ppm. This included FACE-1998_A data for C_r between 340 and 360 ppm and FACE-1998_B A/C_i data for which C_i was nearly as high as the apparent transition point or the next C_i measurement below that. These values of C_i increased with temperature.

Table 1
Parameterization and validation data sets, with external variable ranges.

Name	R_d measured	C_a ppm	Q μmol m^{-2} s^{-1}	Temp °C	RH %	Reference
Parameterization data sets						
FACE-1998_A	no	360, 550	1000–1500	24–36	42–75	Noormets et al., 2001a
FACE-2000	no	1500	0–500	21–29	58–77	Noormets et al., 2010
FACE-1998_B	yes	50–410	1000–1500	19–36	23–81	
Validation data sets						
BOREAS TE-12	yes	70–400	0–2100	15–37	15–33	Arkebauer, 1998
FACE-1999	no	360, 560	1188–1300	17–35	46–77	Noormets et al., 2001b

For parameterization of J_{max}, rather than using A/C_i data in the flat region of the curve well above the transition point, we used data at or near the transition point, where the slope was greater. The J-data consisted of the high-light ($Q \geq 1000$ μmol m^{-2} s^{-1}) portion of the A_j-data set. Although it is possible that some J-data points should have been in the A_c-data instead, there was the benefit of targeting parameterization of A_j directly to a realistic environmental CO_2 concentration range.

2.3. Parameterization procedure

The full parameterization of the [A,g_s]-model was achieved in stages by fitting model components to data using non-linear regression (NLIN Procedure, SAS 8.1; The SAS Institute, Inc., Cary, NC, USA). Prior to parameterization the data were corrected for measurement error due to respiring tissue beneath the gasket as described by Pons and Welschen (2002) and validated for largely heterobaric leaves (Jahnke, 2001). This gasket error occurs when measured respiration is divided by the leaf area within the cuvette chamber, ignoring the portion (assumed to be half) of the leaf-tissue under the gasket which also respired into the chamber. Underestimation of respiring leaf area results in over-estimation of R_d.Based on the LI-6400 leaf cuvette area and gasket thickness, the assumed gasket error was corrected by dividing measured R_d by 1.59. The corresponding corrections to the A and C_i data were made by adding the R_d correction to A and then recalculating C_i using Eq. (6).

The Arrhenius function (3) was fit to the corrected R_d data. Next, V_{cmax} data points were generated using the equation

$$V_{cmax} = \frac{(C_i + K_m)(A + R_d)}{(C_i - \Gamma K_m)}, \quad (8)$$

the V-data, and the R_d, Γ^* and K_m temperature functions. Rather than compute V_{cmax} as the slope of a regression line through three to five points on the A/C_i curve, V_{cmax} was calculated directly from (8). This allowed inclusion of the FACE-1998$_A$ data, where measurements were taken at only a single C_r value per leaf.

The temperature function (4) was fit to the V_{cmax} points. The value of ΔH_d was fixed and then T_{opt}, $V_{cmax,opt}$ and ΔH_a were derived using SAS. As ΔH_d was increased incrementally from 150 000 to 700 000 J mol^{-1} the shape of the resulting peaked function changed from a gently sloping, symmetric bell to an asymmetric one resembling an Arrhenius curve below T_{opt}. Primarily, increasing ΔH_d increased the value of $V_{cmax,opt}$ and the steepness of descent above T_{opt}.

The J points were generated from the equation

$$J = \frac{(4.5C_i + 10.5\Gamma^*)(A + R_d)}{(C_i - \Gamma^*)}, \quad (9)$$

the J-data and the R_d and Γ^* temperature functions. From the J points, J_{max} points were computed according to (5). The temperature dependency function (4) was then fit to the J_{max} points.

The g_s model parameter a_1 was determined by a linear regression fit of the g_s data to the quantity $\frac{A+R_d}{C_i(1+\frac{D_s}{d})}$ using the R_d temperature function and the A, C_i and D_s data in the [A,g_s]-data set for which g_s was at least 0.3 mol m^{-2} s^{-1}.

2.4. Model validation

Common statistical procedures programmed into spreadsheet software were used for model validation. The parameterized R_d, A_c, A_j and [A,g_s] models were first evaluated against the [A,g_s]-data. These data were considered dependent because modeling components were parameterized to subsets of the [A,g_s]-data set. These initial evaluations served as benchmarks for comparisons with independent data.

In addition to visual inspection of data values $X_1, X_2, \ldots X_n$ plotted against their corresponding model-predicted values $Y_1, Y_2, \ldots Y_n$, goodness of fit was assessed based on the slope and R^2 value of the optimal least squares regression line, the root mean squared error ε and the root mean squared relative error ε_r where

$$\varepsilon = \frac{1}{n}\sqrt{\sum_{i=1}^{n}(Y_i - X_i)^2}, \quad (10)$$

$$\varepsilon_r = \frac{1}{n}\sqrt{\sum_{i=1}^{n}\left(\frac{Y_i - X_i}{X_i}\right)^2} \quad (11)$$

The optimal regression line is of the form $y = \alpha x$, where α minimizes the error $\frac{1}{n}\sqrt{\sum_{i=1}^{n}(Y_i - mX_i)^2}$ over all possible slopes m. The quantities ε and ε_r directly measure the error in a model's ability to predict the data points $X_1, X_2, \ldots X_n$.

Two of the data sets in this study had A values ranging from very small to large, but the third data set had only upper-range values of A ($A \geq 15$ μmol m^{-2} s^{-1}). For this reason and to avoid comparing relative error for small A with relative error for large A, we used ε, but not ε_r, to compare the [A,g_s] model's error in predicting A among whole data sets. Both ε and ε_r were reasonable choices for comparison of the [A,g_s] model's error in predicting A over the limited range $A \geq 15$ μmol m^{-2} s^{-1}.

2.5. Validation data

Table 1 lists the independent model validation data sets. The BOREAS TE-12 data were collected from intact leaves of *P. tremuloides* during in 1994 and 1995 at the BOReal Ecosystem-Atmosphere Study near Prince Albert, Saskatchewan at 53.2°N (Arkebauer, 1998). An LI-6200 CO_2 infrared gas analyzer system was used in closed-circuit mode (LI-COR, 1990; McDermitt et al., 1989) with a 14 cm^2 chamber window. The FACE-1999 data were collected in 1999 at the FACTS-II site with an LI-6400 portable open gas exchange system and were measured only at growth C_a levels, approximately 350 and 550 ppm.

In order to validate the model for healthy, mature, sun leaves, the data were filtered in the same manner as the parameterization data. This resulted in data sets for leaves within an LPI range of 9–26, $Q \geq 1000$ μmol m^{-2} s^{-1}, and $A \geq 15$ μmol m^{-2} s^{-1} when $C_r > 300$ ppm. Data for which g_s averaged less than 0.3 mol m^{-2} s^{-1} when C_i was between 145 and 500 ppm were excluded. While the BOREAS TE-12 data were distributed fairly evenly from very low to high values of A, the FACE-1999 data had only $A \geq 15$ μmol m^{-2} s^{-1}.

Additional comparisons were made with Niinemets et al. (1999) LI-6262 open gas exchange system (LI-COR Inc., Lincoln, NE, USA) data collected for upper canopy *Populus tremula* L. leaves in Estonia (latitude 58°22′N). Comparison of R_d results were also made with *P. tremuloides* data from the Aspen FACE site in 2000 (Davey et al., 2004) and 2001 (Singsaas et al., 2003).

3. Results

3.1. R_d, V_{cmax} and J_{max} models

The R_d model is comparable to the Niinemets et al. (1999) R_d model and the BOREAS TE-12 R_d data (Fig. 1, Table 2). The Niinemets et al. (1999) R_d model was fit to data taken over a temperature range of 20–50 °C. Our model predicts $R_d = 1.88$ μmol m^{-2} s^{-1} at 25 °C. In comparison, LI-6400 R_d data at 25 °C reported by Singsaas et al. (2003), when corrected for the gasket error, range from 1.95 to 2.75 μmol m^{-2} s^{-1}, with mean value 2.35 μmol m^{-2} s^{-1}. The range of R_d for aspen published in Davey et al. (2004) is 1.31–1.47 μmol m^{-2} s^{-1} at 25 °C. The Davey et al. (2004) study instrumentation had a cuvette large enough to enclose an entire leaf, avoiding the gasket error.

Because it is proportional to R_d, the R_d gasket error increases with temperature. Thus correcting the error reduces the apparent rise in R_d, and consequently Γ^*, with temperature. It was found that without the R_d correction, Γ^* increased with the slope of Γ^* in Bernacchi et al. (2001) but had lower magnitude. With the R_d correction, Γ^* increased with the slope of Γ^* in Bernacchi et al. (2002) and had similar magnitude.

The V_{cmax} and J points were computed as described in Subsection 2.3 using Eqs. (8) and (9). These data and the R_d data were confirmed by comparison with V_{cmax}, R_d and J_{max} points derived using slope-intercept methods applied to (1) and (2) as described in von Caemmerer (2000).

The V_{cmax} temperature function was fit to the V_{cmax} data (Fig. 2, Table 2). Its value at 25 °C, about 95 μmol m^{-2} s^{-1}, is between the two Singsaas et al. (2003) estimates of V_{cmax} at 25 °C for leaves grown under an ambient CO_2 level of 350 ppm ($V_{cmax} = 80$ μmol m^{-2} s^{-1} estimated from A/C_i data, $V_{cmax} = 102$ μmol m^{-2} s^{-1} estimated from A/C_c data).

An Arrhenius model fit the V_{cmax} data well. All data were apparently for temperatures below T_{opt}. For the peaked function, a deactivation energy of $\Delta H_d = 500\,000$ J mol^{-1} resulted in a fit comparable to an Arrhenius model fit (not shown). Fixing ΔH_d and then applying SAS to simultaneously solve for T_{kopt}, $V_{cmax,opt}$ and ΔH_a resulted in an estimation for T_{kopt} of 38 °C.

Often only A/C_i data well below the cross-over region are used for fitting A_c, as estimation of V_{cmax} could be compromised by accidental inclusion of RuBP regeneration-limited data. Indeed, Dubois et al. (2007) demonstrated that when A_c and A_j are fitted

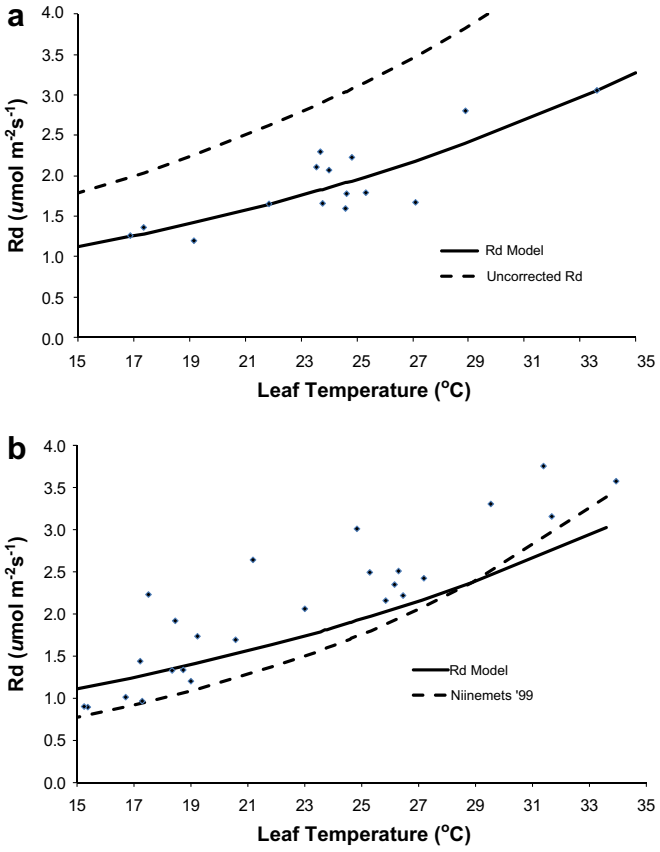

Fig. 1. a) Gasket-corrected R_d data, with R_d model fits to corrected and uncorrected data; b) the R_d model, the Niinemets et al. (1999) R_d model and the BOREAS TE-12 R_d data.

separately using points in or near the cross-over region, the estimates of V_{cmax} and J_{max} can be highly sensitive to the assumed value of the transition point.

In this study, V_{cmax} estimates computed from data near the transition point on the A/C_i curve, for C_i about 300–500 ppm, were nearly the same as the V_{cmax} points obtained from data lower on the A/C_i curve, but not lower than 150 ppm. We hypothesized that using data where $50 < C_i < 100$ ppm would result in lower V_{cmax} points due to CO_2 leakage into the sensor chamber, as well as unmodeled mesophyll conductance (Singsaas et al., 2003; Ethier and Livingston, 2004). However, instead we found only greater variability among the resulting V_{cmax} points.

The J_{max} points and temperature function were compared with J_{max} published in Niinemets et al. (1999) for *P. tremula* (Fig. 3, Table 2). Both J_{max} function values are about 170 μmol m^{-2} s^{-1} at 25 °C, which is lower than the Singsaas et al. (2003) J_{max} values of 216 μmol m^{-2} s^{-1} (for 550 ppm growth CO_2) and 230 μmol m m^{-2} s^{-1} (for 350 ppm growth CO_2) estimated from A/C_i data, and 200 μmol m^{-2} s^{-1} (for 550 ppm growth CO_2) and 217 μmol m^{-2} s^{-1} (for 350 ppm growth CO_2), estimated from A/C_c data.

Table 2
Parameters for temperature models of R_d, V_{cmax}, and J_{max} assuming infinite g_m.

	c	P_{opt} μmol m^{-2} s^{-1}	ΔH_a J mol^{-1}	ΔH_d J mol^{-1}	T_{opt} °C
R_d fit to FACE-1998$_B$ data	16.6	–	39 504	–	–
R_d Niinemets et al. (1999)	23.93	–	57 920	–	–
V_{cmax} fit to A/C_i V-data	–	233.53	59 808	500 000	38
J_{max} fit to A/C_i J-data	–	250.62	33 228	500 000	36
J_{max} Niinemets et al. (1999)	–	380.00	70 600	285 800	34

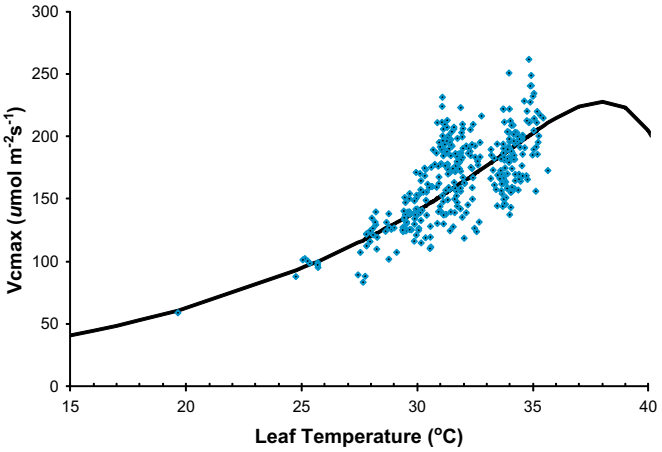

Fig. 2. The V_{cmax} model and the V_{cmax} data, assuming infinite g_m.

3.2. Parameterized g_s and [A,g_s] models

The parameterized g_s model only coarsely predicted the g_s data. Nonetheless, it performed well as a feedback component within the [A,g_s] model. It was expected that the FvCB model would predict the A data better than the [A,g_s] model, since the FvCB model responds to C_i data while the [A,g_s] model responds to C_a. However, for the dependent [A,g_s]-data, predictions of A by the two models differed by no more than 2 μmol m^{-2} s^{-1} when compared over the full range of data, and much less for $A < 15$ μmol m^{-2} s^{-1}.

Analysis of the [A,g_s] model's ability to predict A for the [A,g_s]-data (Fig. 4, Table 3) indicated base-line performance limitations due to some combination of data inaccuracies, parameterization techniques and unmodeled processes contributing to leaf-level photosynthetic rate. Validation with BOREAS TE-12 data (Fig. 5, Table 3) and FACE-1999 data (Fig. 6, Table 3) gave evidence of the [A,g_s] model's ability to predict A for independent data.

Some of the error in predicting the BOREAS TE-12 data may be due to tree age, growth temperature and other environmental differences (Hikosaka et al., 2006). In contrast, the FACE-1999 data were collected at the same site as the parameterization data, only one year later and with water and nutrients not limiting. Thus one might expect better validation results for the FACE-1999 data than for the BOREAS TE-12 data.

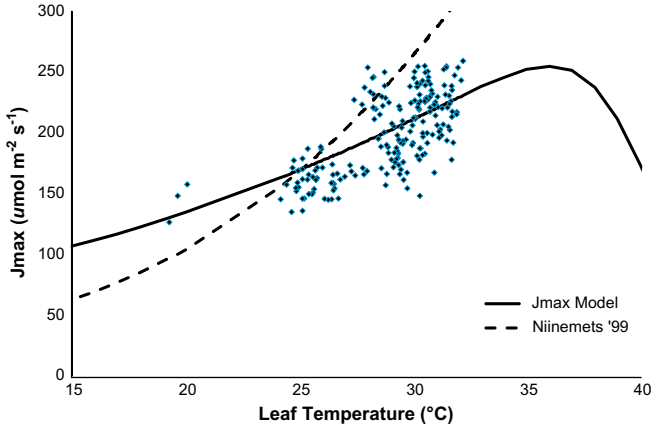

Fig. 3. The J_{max} model, the J_{max} data and the Niinemets et al. (1999) J_{max} model, assuming infinite g_m.

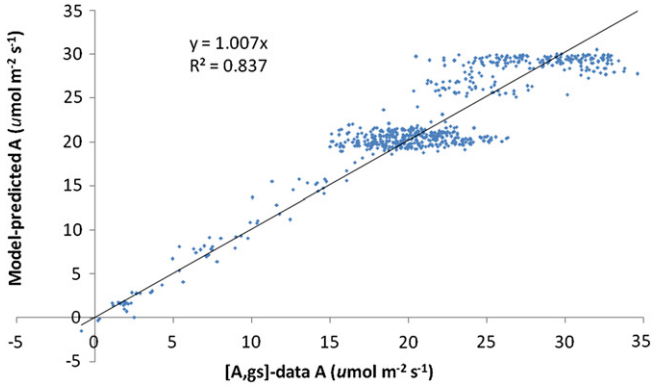

Fig. 4. A predicted by the [A,g_s] model versus LI-COR generated *A* in the [A,g_s]-data.

Both the regression line slope and R^2 values for the FACE-1999 validation were worse than for the BOREAS TE-12 validation (Table 3, column two). However, comparison of these measurements alone can be misleading because the *A* values in the BOREAS TE-12 data range from very low to high, while the FACE-1999 data have only $A \geq 15$ μmol m^{-2} s^{-1}. Limiting the data ranges to $A \geq$ 15 μmol m^{-2} s^{-1} for both the [A,g_s] and BOREAS TE-12 data sets resulted in R^2 values comparable to the R^2 value for the FACE-1999 data set (Table 3, third column).

In terms of ε_r for $A \geq$ 15 μmol m^{-2} s^{-1}, the [A,g_s] model predicted the two independent data sets about equally well and with about 3 times the error than for the dependent data (Table 3 fifth column).

The optimal regression line slope suggests that the [A,g_s] model over-predicts the FACE-1999 *A* data by a factor of 1.219, but the low R^2 value reduces the certainty of this conclusion. The ε measure provides supporting evidence as follows. Let $X_1, X_2, \ldots X_n$ denote the FACE-1999 *A* data points and $Y_1, Y_2, \ldots Y_n$ denote the [A,g_s] model's predictions of these *A* values. The optimal regression line error (see Subsection 2.4) is

$$\varepsilon_{opt} = \frac{1}{n}\sqrt{\sum_{i=1}^{n}(Y_i - 1.219X_i)^2} = 0.131 \ \mu mol\ m^{-2}s^{-1} \qquad (12)$$

This is about 2/5ε. Algebraic manipulation of (12) shows that if the model is scaled so that $A = 1/1.219 \min\{A_c, A_j\}$, it predicts the FACE-1999 *A* data with $\varepsilon = 0.1083$ μmol m^{-2} s^{-1}. This is about as well as the [A,g_s] model, without scaling, predicts the dependent [A,g_s]-data.

3.3. The effects of g_m on apparent V_{cmax} and J_{max}

When V_{cmax} and *J* are estimated from A/C_i data as in Subsection 3.2, it is assumed that g_m is infinite, which is not realistic. To study

Table 3
Quantitative measures of the [A,g_s] model's ability to predict dependent and independent *A* data. The units for A and ε are μmol m^{-2} s^{-1}.

Data set	Regression all *A* data	Regression for $A \geq 15$	Root mean square error ε for all *A*	Root mean square relative error ε_r for $A \geq 15$
[A,g_s]	$y = 1.007x$ $R^2 = 0.837$	$y = 1.007x$ $R^2 = 0.561$	0.105	0.00532
BOREAS TE-12	$y = 1.000x$ $R^2 = 0.887$	$y = 0.953x$ $R^2 = 0.336$	0.136	0.01565
FACE-1999	$y = 1.219x$ $R^2 = 0.543$	$y = 1.219x$ $R^2 = 0.543$	0.310	0.01642

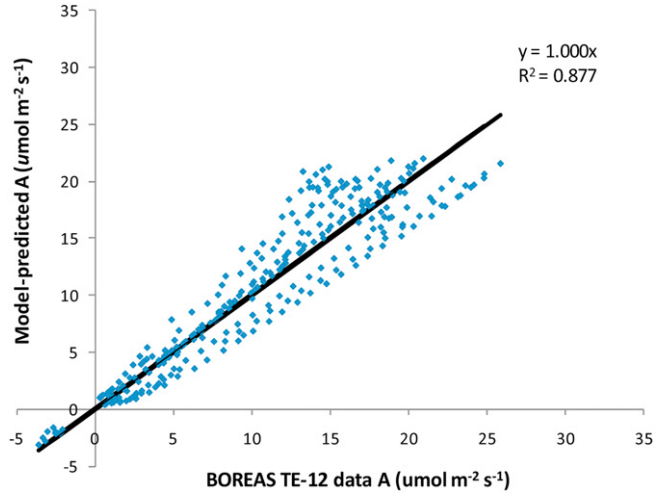

Fig. 5. Validation of the [A,g_s] model with the BOREAS TE-12 data.

the effects of g_m on V_{cmax} and J_{max} we assume that $C_c = C_i - A/g_m$ as in Bernacchi et al. (2002), Flexas et al. (2007), Harley et al. (1992a) and Sharkey et al. (2007) and that $C_i > \Gamma^*$. Replacing C_i in Eqs. (8) and (9) with $C_i - A/g_m$ expresses

V_{cmax} and *J* at the site of Rubisco as functions of g_m. Rearranging terms, we have

$$V_{cmax}(g_m) = \frac{(g_m - r_1)}{(g_m - r_2)}V_{cmax}(\infty), \qquad (13)$$

and

$$J(g_m) = \frac{(g_m - r_3)}{(g_m - r_2)}J(\infty), \qquad (14)$$

where $r_1 = \frac{A}{C_i + K_m}$, $r_2 = \frac{A}{C_i - \Gamma^*}$ and $r_3 = \frac{A}{4.5C_i + 10.5\Gamma^*}$

with $0 < r_1 < r_2 < g_m$ and $0 < r_3 < r_2 < g_m$.

Since $V_{cmax}(g_m)$ and $J_{max}(g_m)$ have vertical asymptotes at $g_m = r_2$, as the value of g_m is reduced toward r_2, $V_{cmax}(g_m)$ and $J(g_m)$ both increase without bound. Also their rates of change with respect to g_m become unbound.

$V_{cmax}(g_m)$ and $J(g_m)$ were investigated using the *V*-data and *J*-data for $g_m = A/b$ for constant *b* ranging from 25 to 170 μmol mol^{-1}.

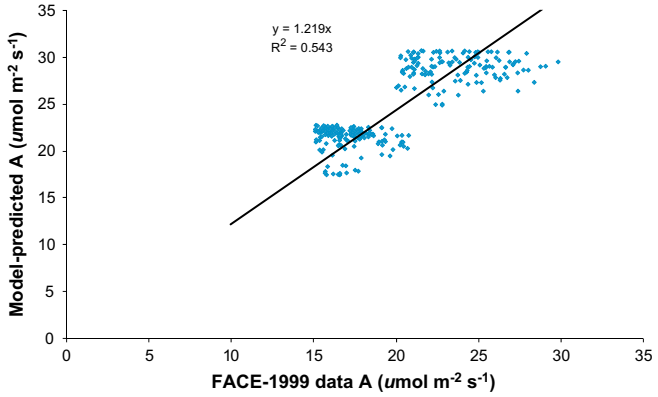

Fig. 6. Validation of the [A,g_s] model with the FACE-1999 data.

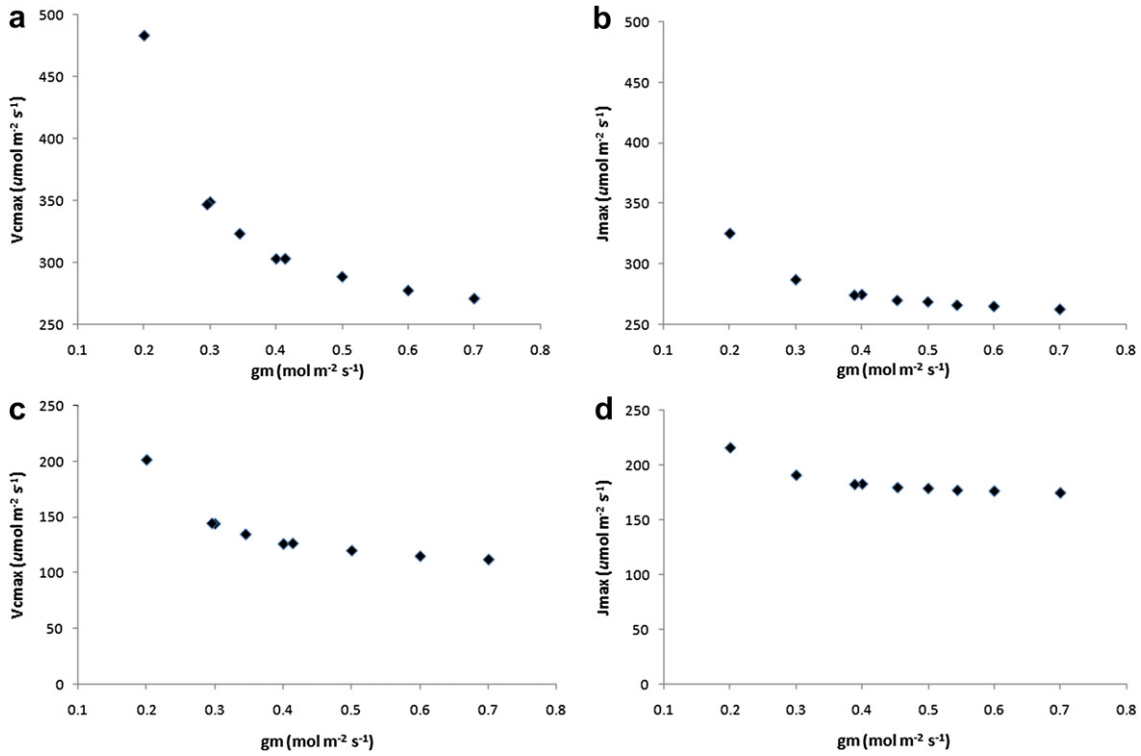

Fig. 7. For g_m assumed to be proportional to A in the V-data and J-data, $\bar{g}_m$ plotted versus a) the parameter $V_{cmax,opt}$, b) the parameter $J_{max,opt}$, c) V_{cmax} at 25 °C, and d) J_{max} at 25 °C.

$V_{cmax}(g_m)$ and $J(g_m)$ points were generated from Eqs. (8) and (9) with C_i replaced by $C_c = C_i - A/g_m = C_i - b$. Temperature function fits of the $V_{cmax}(g_m)$ and $J_{max}(g_m)$ points were achieved by optimizing the coefficients $V_{cmax,opt}$ and $J_{max,opt}$ while maintaining the values of ΔH_a, ΔH_d and T_{opt} given in Table 2. It was found that the difference between $V_{cmax,opt}$ for $\bar{g}_m = 0.20$ mol m^{-2} s^{-1} ($b = 104$ μmol mol^{-1}) and $V_{cmax,opt}$ for $\bar{g}_m = 0.30$ mol m^{-2} s^{-1} ($b = 69$ μmol mol^{-1}) was greater than the difference between $V_{cmax,opt}$ for $\bar{g}_m = 0.30$ mol m^{-2} s^{-1} and $V_{cmax,opt}$ for infinite g_m (Fig. 7). $V_{cmax}(g_m)$ data values rapidly increased and dispersed as $\bar{g}_m$ decreased below 0.20 mol m^{-2} s^{-1} and for $\bar{g}_m < 0.13$ mol m^{-2} s^{-1}, within the range of r_2, some $V_{cmax}(g_m)$ values were huge and negative, some huge and positive and others were undefined.

4. Discussion

4.1. Empirical aspects of the V_{cmax} and J_{max} model components

Comparison of model-predicted A versus the [A,g_s]-data A values verified that the limited V-data and J-data sets were sufficient for parameterizing V_{cmax} and J_{max} to the extent that V_{cmax} and J_{max} were satisfactory internal mathematical components in the [A,g_s] model for predicting leaf-level A. Their effectiveness as components could be further explored by comparing the results in Table 3 with corresponding results obtained for other [A,g_s] models with alternative V_{cmax} and J_{max} functions.

However, V_{cmax} and J_{max} were derived assuming infinite g_m and so do not accurately represent Rubisco dynamics (Niinemets et al., 1999; Singsaas et al., 2003). As shown in Subsection 3.3, assuming finite g_m results in higher estimates of both V_{cmax} and J_{max}. However, even when finite g_m is estimated and included in the FvCB model using the relationship $C_c = C_i - A/g_m$, V_{cmax} and J_{max} derived from A/C_i data can be significantly uncertain. We found that for high g_m, where uncertainty in estimated g_m can be large (Harley et al., 1992a), V_{cmax} and J_{max} changed very little, as also reported by Flexas et al. (2007). However, when g_m is low V_{cmax} and J are very sensitive to uncertainty in g_m. Accurate estimation of g_m may be difficult since, for a variety of C_3 species, g_m changes rapidly and significantly with CO_2 level during A/C_i data collection (Flexas et al., 2007).

The values of V_{cmax} and J_{max} also depend on the values of Γ^* and K_m, generally assumed to be species-independent for C_3 plants (von Caemmerer, 2000). Medlyn et al. (2002) observed sensitivity of V_{cmax} and J_{max} to Γ^* and K_m. In this study, using Bernacchi et al. (2001) kinetics parameters, V_{cmax} assuming infinite g_m was larger than V_{cmax} for finite $\bar{g}_m > 0.7$ mol m^{-2} s^{-1} for the Bernacchi et al. (2002) kinetics parameters (Fig. 8). V_{cmax} increases because the

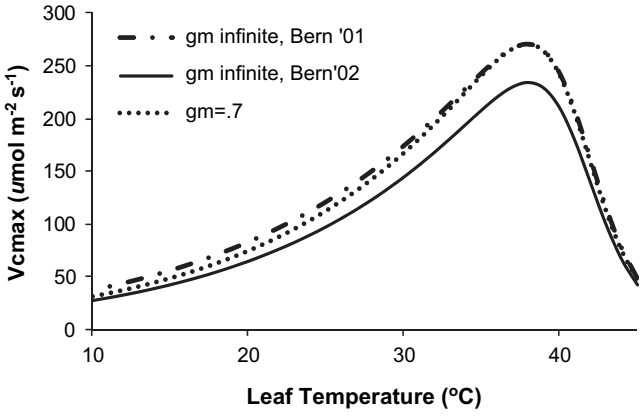

Fig. 8. The models for V_{cmax} assuming infinite g_m and $\bar{g}_m = 0.7$ mol m^{-2} s^{-1}, both derived using the kinetics parameters from Bernacchi et al. (2002), compared to the model for V_{cmax} assuming infinite g_m derived using kinetics parameters from Bernacchi et al. (2001).

Bernacchi et al. (2001) Γ^* and K_m are larger at every temperature than the Bernacchi et al. (2002) Γ^* and K_m. More generally, it is evident from Eq. (8) that with all other terms fixed, V_{cmax} increases with increasing K_m. As Γ^* increases, the positive denominator $(C_i - \Gamma^*)$ in Eq. (8) decreases, which also increases V_{cmax}. When C_i is replaced with C_c in Eq. (8), the same result is evident for V_{cmax} at the site of Rubisco. Thus erroneous conclusions may be drawn from comparison of V_{cmax} from studies using different Γ^* and K_m functions, even if all other aspects of the studies are the same.

4.2. Broader applicability of the analysis methods

The base-line and validation analysis methods of this study can be replicated using simple spreadsheet functions. They can be applied to evaluate and compare various parameterizations and alternative formulations of the [A,g_s] model. For example, one could compare the performance of an [A,g_s] model derived using simultaneous measurements of leaf gas exchange and modulated chlorophyll fluorescence (Long and Bernacchi, 2003; Sharkey et al., 2007) with an [A,g_s] model parameterized using traditional A/C_i techniques. Though the models may differ in source data and parameterization methods, they can be compared as long as they predict A from the same environmental inputs. Similarly, results of different mathematical formulations of components within the [A,g_s] model can be compared. The g_s model of Dewar (2002), for example, responds to leaf water potential as well as humidity. One could use these analysis methods to explore the extent to which substituting a Dewar (2002) g_s model for g_s in Eq. (7) improves an [A,g_s] model's prediction of A data under various water-availability scenarios.

5. Conclusions

This study included parameterization, validation and analysis of a coupled [A,g_s] model of photosynthetic rate for the most productive leaves of *P. tremuloides*. Restricting model parameterization data to limited ranges of environmental variables reduced uncertainty due to measurement limitations at very high and very low chamber C_a and unmodeled changes in internal conditions and mechanisms limiting photosynthetic rate. The model analysis incorporated elementary statistical computations programmed into spreadsheet software.

The analysis methods in this study apply more broadly, irrespective of parameterization techniques and the specific equations of [A,g_s] models. The base-line evaluation with dependent data quantifies the extent to which an [A,g_s] model, its mathematical structure in combination with its parameter values, is able to reproduce a larger body of data from which it was parameterized. This gives a context for assessment of independent validation results. The ε and ε_r measurements complement the graphical and optimal regression line information to facilitate comparison of model validation results for data sets varying in number and distribution of data values.

Acknowledgements

We gratefully acknowledge support from the USDA Northern Global Change Program Forest Service, Award #05-CA-11242343-036, the USDA Forest Service North Central Research Station Integrated Program, Agreement 03-JV-11231300-086, and the Office of Science (BER), U.S. DOE Grant No. DE-FG02-95ER62125. Additional support was provided by the University of Minnesota Duluth's Natural Resources Research Institute and Department of Mathematics and Statistics, and Michigan Technological University.

Appendix

Symbols

A	Steady-state net rate of CO_2 uptake per unit leaf area (μmol m^{-2} s^{-1})
A_c	A limited by Rubisco-catalyzed carboxylation (μmol m^{-2} s^{-1})
A_j	A limited by the regeneration of RuBP controlled by electron transport rate (μmol m^{-2} s^{-1})
a_1	Empirical coefficient (9.5)
c	Scaling constant (dimensionless)
C_a	Atmospheric CO_2 concentration (μmol mol^{-1})
C_c	CO_2 concentration at the site of Rubisco (μmol mol^{-1})
C_i	Intercellular CO_2 concentration (μmol mol^{-1})
C_r	LI-COR, (1990, 2006) reference CO_2 concentration entering the measurement chamber (μmol mol^{-1})
C_s	LI-COR, (1990, 2006) sample CO_2 concentration exiting the measurement chamber (μmol mol^{-1})
D_o	Empirical coefficient (2 kPa)
D_s	Vapor pressure deficit at the leaf surface (kPa)
ΔH_a	Activation energy (J mol^{-1})
ΔH_d	Deactivation energy (J mol^{-1})
E	Transpiration rate per unit leaf area (mol m^{-2} s^{-1})
g_m	CO_2 transfer conductance from the intercellular airspaces of the leaf into the chloroplast, referred to as mesophyll conductance (mol m^{-2} s^{-1})
$\bar{g}_m$	Mean value of g_m (mol m^{-2} s^{-1})
g_s	Stomatal conductance to water vapor (mol m^{-2} s^{-1})
g_{tc}	Total conductance to CO_2(mol m^{-2} s^{-1})
Γ^*	CO_2 compensation point in the absence of dark respiration (μmol mol^{-1})
J	Rate of electron transport (μmol m^{-2} s^{-1})
$J(g_m)$	Estimated J based on finite g_m(μmol m^{-2} s^{-1}).
$J(\infty)$	Estimated J when g_m is assumed to be infinite (μmol m^{-2} s^{-1}).
J_{max}	Maximum rate of electron transport (μmol m^{-2} s^{-1})
$J_{max}(g_m)$	Estimated J_{max} based on finite g_m(μmol m^{-2} s^{-1})
$J_{max}(\infty)$	Estimated J_{max} when g_m is assumed to be infinite (μmol m^{-2} s^{-1})
K_c	Michaelis constant for CO_2 (mmol mol^{-1})
K_o	Michaelis constant for O_2 (mmol mol^{-1})
O_i	Intercellular oxygen concentration (210 mmol mol^{-1})
Q	Photosynthetically active photon flux density (μmol m^{-2} s^{-1})
Q_2	Irradiance absorbed by photosystem II (μmol m^{-2} s^{-1})
R	Molar gas constant (8 314 J K^{-1} mol^{-1})
R_d	Dark (mitochondrial) respiration (μmol m^{-2} s^{-1})
T_c	Leaf temperature in °C
T_k	Leaf temperature in Kelvins
T_{opt}	Optimal leaf temperature in Kelvins
V_{cmax}	Maximum rate of Rubisco carboxylation (μmol m^{-2} s^{-1})
$V_{cmax}(g_m)$	Estimated V_{cmax} based on finite g_m (μmol m^{-2} s^{-1})
$V_{cmax}(\infty)$	Estimated V_{cmax} when g_m is assumed to be infinite (μmol m^{-2} s^{-1})

References

Arkebauer, T.J., 1998. BOREAS TE-12 Leaf Gas Exchange Data. Data Set. Available on-line. Oak Ridge National Laboratory Distributed Active Archive Center, Oak Ridge, Tennessee, USA. http://www.daac.ornl.gov fromdoi:10.3334/ORNLDAAC/351.

Ball, J.T., Woodrow, I.E., Berry, J.A., 1987. A model predicting stomatal conductance and its contribution to the control of photosynthesis under different environmental conditions. In: Biggens, J. (Ed.), Progress in Photosynthesis Research. Martinus Nijhoff Publishers, The Netherlands.

Bernacchi, C.J., Singsaas, E.L., Pimentel, C., Portis, A.R., Long, S.P., 2001. Improved temperature response functions for models of Rubisco-limited photosynthesis. Plant, Cell and Environment 24, 253–259.

Bernacchi, C.J., Portis, A.R., Nakano, H., von Caemmerer, S., Long, S.P., 2002. Temperature response of mesophyll conductance. Implications for the determination of Rubisco enzyme kinetics and for limitations to photosynthesis in vivo. Plant Physiology 130, 1992–1998.

Bernacchi, C.J., Pimentel, C., Long, S.P., 2003. In vivo temperature response functions of parameters required to model RuBP-limited photosynthesis. Plant, Cell and Environment 26, 1419–1430.

von Caemmerer, S., 2000. Techniques in Plant Sciences Volume 2: Biochemical Models of Leaf Photosynthesis. CSIRO Publishing, Collingwood.

Davey, P.A., Hunt, S., Hymus, G.J., DeLucia, E.H., Drake, B.G., Karnosky, D.F., Long, S.P., 2004. Respiratory oxygen uptake is not decreased by an instantaneous elevation of [CO_2], but is increased with long-term growth in the field at elevated [CO_2]. Plant Physiology 134, 520–527.

Dewar, R.C., 2002. The Ball-Berry-Leuning and Tardieu-Davies stomatal models: synthesis and extension within a spatially aggregated picture of guard cell function. Plant, Cell and Environment 25, 1383–1398.

Dickson, R.E., Lewin, K.F., Isebrands, J.G., Coleman, M.D., Heilman, W.E., Riemenschneider, D.E., Sôber, J., Host, G.E., Zak, D.R., Hendrey, G.R., Pregitzer, K.S., Karnosky, D.F., 2000. Forest Atmosphere Carbon Transfer and Storage (FACTS-II) the Aspen Free-air CO_2 and O_3 Enrichment (FACE) Project: an Overview. Gen Tech. Rep. NC-214. Department of Agriculture, Forest Service, North Central Research Station, St. Paul, MN: U.S.

Dubois, J.J.B., Fiscus, E.L., Booker, F.L., Flowers, M.D., Reid, C.D., 2007. Optimizing the statistical estimation of the parameters of the Farquhar-von Caemmerer-Berry model of photosynthesis. New Phytologist 176, 402–414.

Ethier, G.J., Livingston, N.J., 2004. On the need to incorporate sensitivity to CO_2 transfer conductance into the Farquhar-von Caemmerer-Berry leaf photosynthesis model. Plant, Cell and Environment 27, 137–153.

Farquhar, G.D., von Caemmerer, S., 1982. Modeling of photosynthetic responses to environmental conditions. In: Lange, O.L., Nobel, P.S., Osmond, C.B., Ziegler, H. (Eds.), Encyclopedia of Plant Physiology (New Series). Springer-Verlag, Berlin, pp. 549–587.

Farquhar, G.D., von Caemmerer, S., Berry, J.A., 1980. A biochemical model of photosynthetic CO_2 assimilation in leaves of C_3 species. Planta 149, 78–90.

Farquhar, G.D., von Caemmerer, S., Berry, J.A., 2001. Models of photosynthesis. Plant Physiology 125, 42–45.

Farquhar, G.D., Sharkey, T.D., 1982. Stomatal conductance and photosynthesis. Annual Reviews of Plant Physiology 33, 317–345.

Flexas, J., Diaz-Espejo, A., Galmes, J., Kaldenhoff, R., Medrano, H., Ribas-Carbo, M., 2007. Rapid variations of mesophyll conductance in response to changes in CO_2 concentration around leaves. Plant, Cell and Environment 30, 1284–1298.

Flexas, J., Ribas-Carbo, M., Diaz-Espejo, A., Galmes, J., Medrano, H., 2008. Mesophyll conductance to CO_2: current knowledge and future prospects. Plant, Cell and Environment 31, 602–621.

Harley, P.C., Loreto, F., Di Marco, G., Sharkey, T.D., 1992a. Theoretical considerations when estimating the mesophyll conductance to CO_2 flux by analysis of the response of photosynthesis to CO_2. Plant Physiology 98, 1429–1436.

Harley, P.C., Thomas, R.B., Reynolds, J.F., Strain, B.R., 1992b. Modeling photosynthesis of cotton grown in elevated CO_2. Plant, Cell and Environment 15, 271–282.

Harley, P.C., Tenhunen, J.D., 1991. Modeling the photosynthetic response of C_3 leaves to environmental factors. In: Boote, K.J., Loomis, R.S. (Eds.), Modeling Crop Photosynthesis – from Biochemistry to Canopy. Crop Science of America, Madison, pp. 17–39.

Hikosaka, K., Ishikawa, K., Borjigidal, A., Muller, O., Onoda, Y., 2006. Temperature acclimation of photosynthesis: mechanisms involved in the changes in temperature dependence of photosynthetic rate. Journal of Experimental Botany 57 (No. 2), 291–302.

Jahnke, S., 2001. Atmospheric CO_2 concentration does not directly affect leaf respiration in bean or poplar. Plant, Cell and Environment 24, 1139–1151.

Karnosky, D.F., Zak, D.R., Pregitzer, K.S., Awmack, C.S., Bockheim, J.G., Dickson, R.E., Hendrey, G.R., Host, G.E., Jones, W.S., King, J.S., Kopper, B.J., Kruger, E.L., Kubiske, M.E., Lindroth, R.L., Mattson, W.J., McDonald, E.P., Noormets, A., Oksanen, E., Parsons, W.F.J., Percy, K.E., Podila, G.K., Riemenschneider, D.E., Sharma, P., Sôber, A., Sôber, J., Anttonen, S., Vapaavuori, E., Isebrands, J.G., 2003. Tropospheric O_3 moderates responses of temperate hardwood forests to elevated CO_2: a synthesis of molecular to ecosystem results from the Aspen FACE project. Functional Ecology 17, 289–304.

Kim, S.H., Lieth, J.H., 2003. A coupled model of photosynthesis, stomatal conductance and transpiration for a rose leaf (*Rosa hybrida* L.). Annals of Botany 91, 771–781.

Kubiske, M.E., Zak, D.R., Pregitzer, K.S., Takeuchi, Y., 2002. Photosynthetic acclimation of overstory *Populus tremuloides* and understory *Acer saccharum* to elevated atmospheric CO_2 concentration: interactions with shade and soil nitrogen. Tree Physiology 22, 321–329.

Kull, O., Sôber, A., Coleman, M.D., Dickson, R.E., Isebrands, J.G., Gagnon, Z., Karnosky, D.F., 1996. Photosynthetic responses of aspen clones to simultaneous exposures of O_3 and CO_2. Canadian Journal of Forestry Research 26, 639–648.

Leuning, R., 1995. A critical appraisal of a combined stomatal-photosynthesis model for C_3 plants. Plant, Cell and Environment 18, 339–355.

LI-COR, 1990. LI-6200 Technical Reference Manual. LI-COR, Inc, Lincoln, NE, USA.

LI-COR, 1998. Using the LI-6400 Portable Photosynthesis System, second ed. LI-COR, Inc, Lincoln, NE, USA.

LI-COR, 2006. Using the LI-6400 Portable Photosynthesis System. Version 5. http://www.licor.com/env/Products/li6400/6400_manuals.jsp

Long, S.P., Bernacchi, C.J., 2003. Gas exchange measurements, what can they tell us about the underlying limitations to photosynthesis? Procedures and sources of error. Journal of Experimental Botany 54 (No. 392), 2393–2401.

Long, S.P., Farage, P.K., Garcia, R.L., 1996. Measurement of leaf and canopy photosynthetic CO_2 exchange in the field. Journal of Experimental Botany 47, 1629–1642.

Martin, M.J., Farage, P.K., Humphries, S.W., Long, S.P., 2000. Can the stomatal changes caused by acute ozone exposure be predicted by changes occurring in the mesophyll? A simplification for models of vegetation response to the global increase in tropospheric elevated ozone episodes. Australian Journal of Plant Physiology 27, 211–219.

Martin, M.J., Host, G.E., Lenz, K.E., Isebrands, J.G., 2001. Simulating the growth response of aspen to elevated ozone: a mechanistic approach to scaling a leaf-level model of ozone effects on photosynthesis to a complex canopy architecture. Environmental Pollution 115, 425–436.

McDermitt, D.K., Norman, J.M., Davis, J.T., Ball, T.M., Arkebaurer, T.J., Welles, J.M., Roemer, S.R., 1989. CO_2 response curves can be measured with a field-portable closed-loop photosynthesis system. Annals of Forestry Sciences (Suppl. 46), 416s–420s.

Medlyn, B.E., Dreyer, E., Ellsworth, D., Forstreuter, M., Harley, P.C., Kirschbaum, M.U.F., Le Roux, X., Montpied, P., Strassemeyer, J., Walcroft, A., Wang, K., Loustau, D., 2002. Temperature response of parameters of a biochemically based model of photosynthesis. II. A review of experimental data. Plant, Cell and Environment 25, 1167–1179.

Mott, K.A., Buckley, T.N., 2000. Patchy stomatal conductance: emergent collective behaviour of stomata. Trends in Plant Science 5 (6), 258–262.

Niinemets, Ü, Oja, V., Kull, O., 1999. Shape of leaf photosynthetic electron transport versus temperature response curve is not constant along canopy light gradients in temperate deciduous trees. Plant, Cell and Environment 22, 1497–1513.

Niinemets, Ü, Cescatti, A., Rodeghiero, M., Tosens, T., 2005. Leaf internal diffusion conductance limits photosynthesis more strongly in older leaves of Mediterranean evergreen broad-leaved species. Plant, Cell and Environment 28, 1552–1566.

Noormets., A., Sôber, A., Pell, E.J., Dickson, R.E., Podila, G.K., Sôber, J., Isebrands, J.G., Karnosky, D.F., 2001a. Stomatal and non-stomatal limitation to photosynthesis in two trembling aspen (*Populus tremuloides Michx.*) clones exposed to elevated CO_2 and/or O_3. Plant, Cell and Environment 24, 327–336.

Noormets, A., McDonald, E.P., Dickson, R.E., Kruger, E.L., Sôber, A., Isebrands, J.G., Karnosky, D.F., 2001b. The effect of elevated carbon dioxide and ozone on leaf- and branch-level photosynthesis and potential plant-level carbon gain in aspen. Trees 15, 262–270.

Noormets, A., Kull, O., Sôber, A., Kubiske, M.E., Karnosky, D.F., 2010. Elevated CO_2 response of photosynthesis depends on ozone concentration in aspen. Environmental Pollution 158, 992–999.

Pons, T.L., Welschen, R.A.M., 2002. Overestimation of respiration rates in commercially available clamp-on leaf chambers. Complications with measurement of net photosynthesis. Plant, Cell and Environment 25, 1367–1372.

Reich, P.B., 1983. Effects of low concentration of O_3 on net photosynthesis, dark respiration, and chlorophyll contents in aging hybrid poplar leaves. Plant Physiology 73, 291–296.

Rodeghiero, M., Niinemets., Ü, Cescatti, A., 2007. Major diffusion leaks of clamp-on leaf cuvettes still unaccounted: how erroneous are the estimates of Farquhar et al. model parameters? Plant, Cell and Environment 30, 1006–1022.

Rogers, A., Humphries, S.W., 2000. A mechanistic evaluation of photosynthetic acclimation at elevated CO_2. Global Change Biology 6, 1005–1011.

Schultz, H.R., 2003. Extension of a Farquhar model for limitations of leaf photosynthesis induced by light environment, phenology and leaf age in grapevines (*Vitis vinifera* L. cvv. White Riesling and Zinfandel). Functional Plant Biology 30, 673–687.

Schurr, U., Walter, A., Rascher, U., 2006. Functional dynamics of plant growth and photosynthesis – from steady-state to dynamics – from homogeneity to heterogeneity. Plant, Cell and Environment 29, 340–352.

Sharkey, T.D., 1985. Photosynthesis in intact leaves of C_3 plants: physics, physiology and rate limitations. The Botanical Review 51, 53–105.

Sharkey, T.D., Bernacchi, C.J., Farquhar, G.D., Singsaas, E.L., 2007. Fitting photosynthetic carbon dioxide response curves for C_3 leaves. Plant, Cell and Environment 30, 1035–1040.

Singsaas, E.L., Ort, D.R., Delucia, E.H., 2003. Elevated CO_2 effects on mesophyll conductance and its consequences for interpreting photosynthetic physiology. Plant, Cell and Environment 27, 41–50.